Article ID: 1007－4627(2006)04－0387－10

Formation Mechanism of Super Heavy Nuclei in Heavy-ion Collisions*

LI Jun-qing[1,2], ZUO Wei[1,2], FENG Zhao-qing[1], JIN Gen-ming[1,2], ZHAO En-guang[2,3]

(1 *Institute of Modern Physics, Chinese Academy of Sciences, Lanzhou* 730000, *China*;
2 *Center of Theoretical Nuclear Physics, National Laboratory of Heavy Ion Accelerator of Lanzhou, Lanzhou* 730000, *China*;
3 *Institute of Theoretical Physics, Chinese Academy of Sciences, Beijing* 100080, *China*)

Abstract: In the dinuclear system conception, the master equation is solved numerically to calculate the fusion probabilities of super-heavy nuclei. The relative motion concerning the energy, the angular momentum and the fragment deformation relaxations is explicitly treated to couple with the diffusion process. The nucleon transition probabilities, which are derived microscopically, are related with the energy dissipation of the relative motion, thus they are time-dependent. The formation cross sections of the super-heavy nuclei from Pb-based cold fusion and excitation functions from ^{48}Ca induced hot fusion are reasonably consistent with known experimental data.

Key words: super heavy-nuclei; dinuclear system; driving potential; master equation; complete fusion

CLC number: O571.6 **Document code**: A

1 Introduction

The great success on the synthesizing super-heavy nuclei(SHN) is very intriguing, and has received much attention[1,2]. The theoretical prediction has shown that there exists a next doubly magic shell closure beyond ^{208}Pb. However the further progress becomes more and more difficult because the formation cross sections are very small, and the excitation functions are very narrow. A better understanding of the physical conception on the SHN is needed, and the mechanism of the fusion dynamics of heavy nuclei is not yet completely clear. Several models are developed to explore the mechanism leading to SHE[3—9], among them the concept of the dinuclear system (DNS) is one of a few models so far which gives no contradiction to the available experimental data.

Based on the DNS conception, and on the former transport theory of deeply inelastic collisions[10,11], a master equation (ME) is obtained, and is solved numerically to treat the nucleon transfer between the colliding nuclei, and to obtain the fusion probability. In the ME, the nucleon transition probabilities, which are derived microscopically, are related with the energy dissipation of the relative motion, thus they are time-dependent. Different from the treatment by Adamian et al[6,12—14], the harmonic oscillator approximation of the potential energy surface which contains shell structure and even-odd corrections, has been avoi-

* **Received date**: 28 Sep. 2006
* **Foundation item**: National Natural Science Foundation of China (10505016, 10235020, 10475099, 10375001); Knowledge Innovation Project of Chinese Academy of Sciences (KJCX2-SW-No17); Financial Support from DFG of Germany
Biography: Li Junqing (1941－), female(Han Nationality), Xiaoshan, Zhejiang, Professor, currently working on the theory about the super-heavy nucleus; E-mail: jqli@impcas.ac.cn

ded by solving the ME numerically in our treatment. And the diffusion process is coupled with the relative motion[15—17]. Based on the fusion probability obtained from the numerical solution of the ME, together with the calculated survival probabilities, the evaporation residue cross sections are obtained. By introducing the barrier distribution function method in the DNS model, the fusion-evaporation excitation functions of some SHN produced by the ^{48}Ca induced reactions can well reproduce the data.

In section 2 the basic theory is introduced. In section 3, the formation cross sections of SHN from Pb-based cold fusion and the excitation function from ^{48}Ca induced hot fusion are shown. Our summary is given in section 4.

2 The DNS Conception

In the DNS concept the evaporation residue cross section can be written as a sum over all partial waves J[12]

$$\sigma_{\mathrm{ER}}(E_{\mathrm{cm}}) = \sum_{J=0}^{J=J_{\mathrm{f}}} \sigma_{\mathrm{c}}(E_{\mathrm{cm}},J)\ P_{\mathrm{CN}}(E_{\mathrm{cm}},J)\cdot W_{\mathrm{sur}}(E_{\mathrm{cm}},J)\ , \tag{1}$$

where σ_{c} is the capture cross section, P_{CN} is the fussion probability and W_{sur} is the survival probability.

2.1 The partial capture cross section

In Eq. (1) the partial capture cross section for the transition of the colliding nuclei over the entrance barrier with the transmission probability $T(E_{\mathrm{cm}},J)$ at the incident energy of center of mass E_{cm} to form the DNS is given by

$$\sigma_{\mathrm{c}}(E_{\mathrm{cm}},J) = \pi\lambda\!\!\!^{-2}(2J+1)T(E_{\mathrm{cm}},J)\ , \tag{2}$$

in which $\lambda\!\!\!^{-}$ is the reduced de Broglie wavelength, $\lambda\!\!\!^{-2} = \hbar^2/(2\mu E_{\mathrm{cm}})$, with μ the reduced mass. The transmission probability is given by

$$T(E_{\mathrm{cm}},J) = \int f(B)\cdot \frac{1}{1+\exp\left\{\frac{2\pi}{\hbar\omega_B(J)}\left[B+\frac{J(J+1)\hbar^2}{2\mu R_B^2(J)}-E_{\mathrm{cm}}\right]\right\}}\mathrm{d}B\ , \tag{3}$$

where B represents the Coulomb barrier, R_B the position of the barrier, and $\hbar\omega_B$ is defined by the width of the parabolic barrier. The barrier distribution function is taken as asymmetric Gaussian form $f(B) = \frac{1}{N}\exp\left[-\left(\frac{B-B_{\mathrm{m}}}{\Delta_1}\right)^2\right]$ $(B<B_{\mathrm{m}})$ and $f(B) = \frac{1}{N}\exp\left[-\left(\frac{B-B_{\mathrm{m}}}{\Delta_2}\right)^2\right]$ $(B>B_{\mathrm{m}})$ with $B_{\mathrm{m}} = (B_0+B_{\mathrm{s}})$ as in Ref. [7]. B_0 and B_{s} are the height of the Coulomb barrier at waist-to-waist orientation and the height of the minimum barrier with variance of dynamical deformation β_1 and β_2, respectively. N is the normalization constant, $\Delta_2 = (B_0-B_{\mathrm{s}})/2$. The value of Δ_1 is several MeV less than the value of Δ_2, usually it is taken as 2—4 MeV.

The nucleus-nucleus interaction potential with quadrupole deformations in the calculation is taken as the form

$$V(r,\beta_1,\beta_2,\theta_1,\theta_2) = V_{\mathrm{C}}(r,\beta_1,\beta_2,\theta_1,\theta_2) + V_{\mathrm{N}}(r,\beta_1,\beta_2,\theta_1,\theta_2) + \frac{1}{2}C_1(\beta_1-\beta_2^0) + \frac{1}{2}C_2(\beta_1-\beta_2^0)\ . \tag{4}$$

Here the sign 1 and 2 stand for the projectile and target, $\beta_{1,2}$ are the parameters of dynamical deformation, $\beta_{1,2}^0$ are the parameters of static deformation, $\theta_{1,2}$ are the angles between radius vector $\boldsymbol{r}$ and the symmetry axes of statically deformed nuclei, and $C_{1,2}$ are the stiffness parameters, which are calculated within the liquid drop model. $V_{\mathrm{C,N}}$ will be given afterwards. For cold fusion, the energies E_{cm} is near above the Coulomb barrier, $T(E_{\mathrm{cm}},J)\simeq 0.5$ are chosen for partial waves considered.

2.2 The fusion probability

The probability $P_{\mathrm{CN}}(E_{\mathrm{cm}},J)$ of the complete fusion is evaluated by considering the fusion

process as a diffusion of DNS in the mass asymmetry $\eta=(A_1-A_2)/A$, with A_1, A_2 the mass numbers of the DNS nuclei, and $A=A_1+A_2$. Let $P(A_1,E_1,t)$ be the distribution function to find A_1 nucleons with excitation energy E_1 in fragment 1 at time t, where E_1 is not considered as an independent variable but a parameter supplied by the initial relative motion. $P(A_1,E_1,t)$ obeys the following ME:

$$\frac{\mathrm{d}P(A_1,E_1,t)}{\mathrm{d}t}=\sum_{A_1'}W_{A_1,A_1'}\left[d_{A_1}P(A_1',E_1',t)-d_{A_1'}P(A_1,E_1,t)\right]-\Lambda^{\mathrm{qf}}_{A_1,E_1,t}(\Theta)P(A_1,E_1,t)\ , \tag{5}$$

where $W_{A_1,A_1'}=W_{A_1',A_1}$ is the mean transition probability from a channel $(A_1,\ E_1)$ to $(A_1',\ E_1')$, d_{A_1} denotes the microscopic dimension for the corresponding macroscopic variables. The coefficient $\Lambda^{\mathrm{qf}}_{A_1,E_1,t}(\Theta)$ is the rate of decay probability in R, and will be described later. The sum is taken over all possible mass numbers that fragment 1 may take(from 0 to $A=A_1+A_2$). The motion of the nucleons in the interacting nuclei is considered to be described by the single-particle Hamiltonian[10,11]

$$H(t)=H_0(t)+V(t) \tag{6}$$

with

$$H_0(t)=\sum_k\sum_{\nu_k}\varepsilon_{\nu_k}(t)a^{\dagger}_{\nu_k}(t)a_{\nu_k}(t)\ , \tag{7}$$

$$V(t)=\sum_{k,k'}\sum_{\alpha_k,\beta_{k'}}u_{\alpha_k\beta_{k'}}(t)a^{\dagger}_{\alpha_k}(t)a_{\beta_{k'}}(t)=\sum_{k,k'}V_{k,k'}(t),\quad k,k'=1,2\ . \tag{8}$$

The quantities $\varepsilon_\nu(t)$ and $u_{\nu\mu}(t)$ denote the single-particle energies and the interaction matrix elements, respectively. The single-particle states are defined with respect to the moving centers of nuclei and are assumed to be orthogonalized in the overlap region. Therefore, the annihilation and creation operators depend on time. The single-particle interaction matrix element is parameterized by

$$u_{\alpha_k\beta_{k'}}(t)=U_{kk'}(t)\cdot\left\{\exp\left[-\frac{1}{2}\left(\frac{\varepsilon_{\alpha_k}(t)-\varepsilon_{\beta_{k'}}(t)}{\Delta_{kk'}(t)}\right)^2\right]-\delta_{\alpha_k,\beta_{k'}}\right\}\ , \tag{9}$$

which contain some fixed independent parameters $U_{kk'}(t)$ and $\Delta_{kk'}(t)$. These parameters, the calculation of the mean transition probabilities, as well as the procedure to solve the ME were described in Refs. [10,11,15] and references therein except that the quasi-fission effects were not considered there.

The local excitation energy, which provides the excitation energy for the mean transition probability, i. e., for the nucleon transfer, is defined as:

$$\varepsilon^*=E-U(A_1,A_2)\ , \tag{10}$$

where E is the intrinsic excitation energy of the composite system converted from the relative kinetic energy loss, which is determined for each initial relative angular momentum J by the parametrization method of the classical deflection function[18].

The potential energy of the DNS, i. e., the driving potential energy for the nucleon transfer of the DNS is:

$$U(A_1,A_2)=B(A_1)+B(A_2)-\left[B(A)+V'_{\mathrm{rot}}(J)\right]+U_{\mathrm{C}}(A_1,A_2)+U_{\mathrm{N}}(A_1,A_2)+V_{\mathrm{rot}}(J)\ , \tag{11}$$

where $B(A_1)$, $B(A_2)$, and $B(A)$ are the binding energies of the fragments and compound nucleus, respectively, and are taken from Ref. [19], so that the shell and paring corrections are included in them. $U_{\mathrm{C}}(A_1,A_2)$, $U_{\mathrm{N}}(A_1,A_2)$, and $V_{\mathrm{rot}}(J)$ are the Coulomb, nuclear, and centrifugal parts of the nucleus-nucleus potential, respectively.

If the ground state deformations of the two touching nuclei are taken into account, and if the symmetry axis of the two nuclei are in the same plane, the Coulomb interaction of the deformed DNS, $U_{\mathrm{C}}(A_1,\ A_2)$, can be expressed by an analytical formula[20]:

$$U_{\mathrm{C}}(R,\theta)=\frac{Z_1Z_2e^2}{R}+\left(\frac{9}{20\pi}\right)^{1/2}\left(\frac{Z_1Z_2e^2}{R^3}\right)\cdot$$

$$\sum_{i=1}^{2}\mathscr{R}_i^2\beta_2^{(i)}P_2(\cos\theta_i)+\left(\frac{3}{7\pi}\right)^{1/2}\left(\frac{Z_1Z_2e^2}{R^3}\right)\cdot\sum_{i=1}^{2}\mathscr{R}_i^2[\beta_2^{(i)}P_2(\cos\theta_i)]^2 \quad , \tag{12}$$

where θ_i is the angle measured between the radius vector $\boldsymbol{R}$ and the symmetry axis of the i-th nucleus. $\mathscr{R}_i$ is the radius of the deformed nucleus i. In the case of the pole to pole orientation, $\theta_i=0$.

By adopting a Skyrme-type interaction without considering the momentum and spin dependence, the nuclear potential energy is formulated as follows:

$$U_N(R)=C_0\left\{\frac{F_{in}-F_{ex}}{\rho_{00}}\left[\int\rho_1^2(\boldsymbol{r})\rho_2(\boldsymbol{r}-\boldsymbol{R})\mathrm{d}\boldsymbol{r}+\int\rho_1(\boldsymbol{r})\rho_2^2(\boldsymbol{r}-\boldsymbol{R})\mathrm{d}\boldsymbol{r}\right]+F_{ex}\int\rho_1(\boldsymbol{r})\rho_2(\boldsymbol{r}-\boldsymbol{R})\mathrm{d}\boldsymbol{r}\right\} \tag{13}$$

with

$$F_{in,ex}=f_{in,ex}+f'_{in,ex}\frac{N_1-Z_1}{A_1}\frac{N_2-Z_2}{A_2} \quad . \tag{14}$$

where a zero-range treatment of the effective interaction $\delta(\boldsymbol{r}_1-\boldsymbol{r}_2)$ is assumed. The nuclear potential is obtained in the sudden approximation[21]. $N_{1,2}$ and $Z_{1,2}$ are the neutron and proton numbers of the two nuclei, respectively. The parameters $C_0=300$ MeV·fm^3, $f_{in}=0.09$, $f_{ex}=-2.59$, $f'_{in}=0.42$, $f'_{ex}=0.54$, and $\rho_{00}=0.17$ fm^{-3} are used. The functions ρ_1 and ρ_2 are two-parameter (the deformation parameter and the diffuseness) Woods-Saxon density distributions.

The evolution of the DNS in the variable R of the relative distance between the centers of the interacting nuclei will lead to quasi-fission of the DNS. For a given mass asymmetry η, the nucleus-nucleus interaction potential as a function of R is:

$$V(A_1,A_2,R)=U_C(A_1,A_2,R)+U_N(A_1,A_2,R)+U_{rot}(A_1,A_2,R) \quad , \tag{15}$$

where U_C and U_N is calculated by Eq. (12) and Eq. (13), respectively, as a function of R at each combination of the DNS. U_{rot} is the centrifugal potential. The nucleus-nucleus interaction potential $V(A_1,A_2,R)$ has a pocket as a function of the relative distance R with a small depth which results from the attractive nuclear and repulsive Coulomb interactions. The probability $P(A_1,E_1,t)$ distributed in the pocket will have the chance to decay out of the pocket with a decay rate $\Lambda^{qf}_{A_1,E_1,t}(\Theta)$ in Eq. (5), which can be treated with the one dimensional Kramers rate as in Refs. [22,23]:

$$\Lambda^{qf}_{A_1,E_1,t}(\Theta)=\frac{\omega}{2\pi\omega^{B_{qf}}}\left[\sqrt{\left(\frac{\Gamma}{2\hbar}\right)^2+(\omega^{B_{qf}})^2}-\frac{\Gamma}{2\hbar}\right]\cdot\exp\left[-\frac{B_{qf}(A_1)}{\Theta(A_1,E_1,t)}\right] \quad , \tag{16}$$

which depends exponentially on the quasi fission barrier $B_{qf}(A_1)$ for a given mass asymmetry η, and the $B_{qf}(A_1)$ measures the depth of this pocket. The temperature $\Theta(A_1,E_1,t)$ is calculated by using the Fermi-gas expression $\Theta=\sqrt{\varepsilon^*_1/a}$ corresponding to the excitation energy of Eq. (10), and $a=A/12$ MeV^{-1}. $\omega^{B_{qf}}$ in Eq. (16) is the frequency of the inverted harmonic oscillator approximating the potential V in R around the top of the quasi fission barrier. And ω is the frequency of the harmonic oscillator approximating the potential in R at the bottom of the pocket. They are determined by the local oscillator approximation of the nucleus-nucleus potential energy. From our calculation, the extracted average values are $\hbar\omega^{B_{qf}}\approx 2.0$ MeV, and $\hbar\omega\approx 4.0$ MeV. The quantity Γ denotes a double average width of the contributing single-particle states, which determines the friction coefficients:

$$\gamma_{ii'}=\frac{\Gamma}{\hbar}\mu^{-1}_{ii'} \quad ,$$

with $\mu_{ii'}$ the mass parameters. And $\Gamma\approx 2$ MeV.

The calculated driving potentials for the systems ^{76,82}Ge $+^{208}$Pb$\rightarrow{}^{284,290}$114 are shown in Fig. 1 as a function of the mass asymmetry variable $\eta=(A_1-A_2)/(A_1+A_2)$ with thick line and thin doted line, respectively. In the figure the arrow (η_i) points to the incident channel. One nucleon transfers from η_i to both sides, whether it is a neutron or a proton, depending on which would make the potential energy lower. Consequently, the driving

potential of Eq. (11) is an explicit function of neutron and proton numbers of the fragments. One may find out that in order to form a compound nucleus, a barrier $B^*_{\rm fus}$ shown in the figure must be overcome, and the energy needed to pass over the barrier must be supplied by the incident energy. The survival probability of the compound nucleus demands the lowest excitation energy, so the optimal excitation energy indicated in the figure is $E^*_{\rm CN}=U(\eta_i)+B^*_{\rm fus}$ where $U(\eta_i)$ is the potential energy of the initial DNS. In the figure the ground state deformation β_2 of the nuclei of the DNS is taken from Ref. [19]. The orientation of the deformed nuclei and the distance between the centers of the two nuclei are taken in a way which gives the lowest nucleus-nucleus interaction energy.

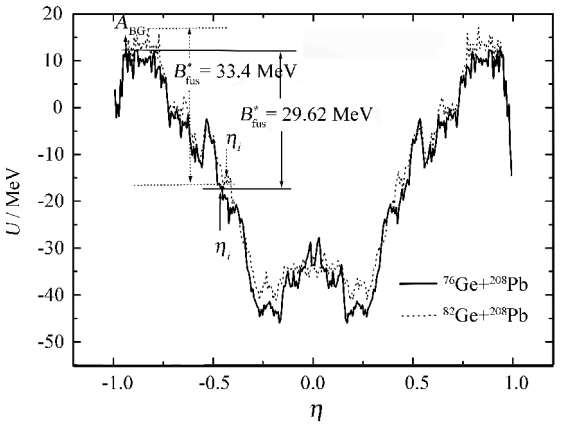

Fig. 1 The driving potential of the DNS for the system ^{76,82}Ge + ^{208}Pb→ ^{284,290}114 as a function of the mass asymmetry variable η. $A_{\rm BG}$ marks the top point of the potential energy.

Solving the Master equation Eq. (5) numerically, the time evolution of $P(A_k, E_k, t)$ to find fragment k (mass number A_k) with excitation energy E_k at time t is obtained. All the components on the left side of the inner fusion barrier in Fig. 1 contribute to the compound nuclear formation. The fusion probability $P_{\rm CN}$ is the summation from $A_1=0$ to $A_{\rm BG}$:

$$P_{\rm CN}(J)=\int_{A_1=0}^{A_{\rm BG}} P(A_1, E_k(J), \tau_{\rm int}(J))\,{\rm d}A_1 \ . \tag{17}$$

Fig. 2(a) shows the calculated values of $P_{\rm CN}$ for Pb-based reactions at nearly central collisions ($J\approx 0$) and with the reaction energies according to those optimal excitation energies for one neutron emission of cold fusion. Full dots are calculated results by Eq. (5) without considering the quasi fission. Open triangles are those including the quasi fission. One may find that $P_{\rm CN}$ with the consideration of the quasi fission decreases by about four orders of magnitude with Z increasing from 106 to 118. Because the inner fusion barrier $B^*_{\rm fus}$ increases

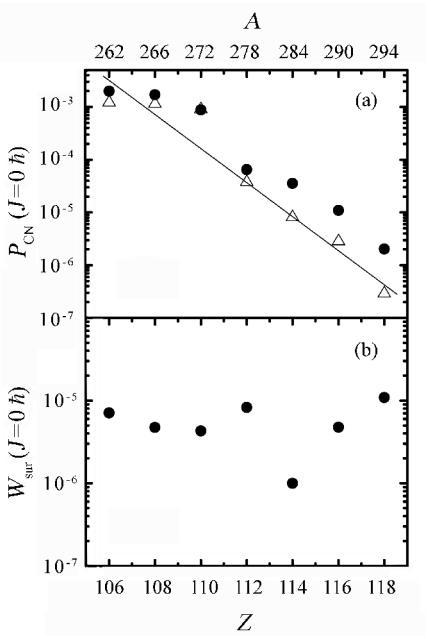

Fig. 2 (a) the calculated values of the fusion probability $P_{\rm CN}$ for one-neutron emission Pb-based reactions at nearly central collisions and with the optimal reaction energies as a function of the charge number of the compound nuclei. The open triangles and solid dots stand for the fusion probability $P_{\rm CN}$ with and without considering the effect of the quasi fission, respectively. The corresponding mass number are listed on the top row. (b) the corresponding calculated survival probability.

with decreasing mass asymmetry of the initial DNS, i. e., with increasing Z for the Pb-based reactions, the fusion probabilities decrease rapidly with increasing Z. The straight line in the figure is used to guide the eye. The consideration of the quasi fission process in the ME diminishes the fusion probability by one order of magnitude for Kr

+Pb→ 118. The decreasing magnitude of the fusion probability becomes less and less as increasing the asymmetry of the incident reaction system, since the inner fusion barrier is getting decreasing, and the distribution probability gets less chance to go to mass symmetrical direction, to which the quasi fission barrier is getting smaller.

2.3 The survival probability of excited compound nucleus

The super-heavy compound nuclei are formed in the excited states, and will lose excitation energy mainly by emission of particles and γ quanta, and by fission. The survival probability estimates the competition between fission and particle emission in the excited compound nucleus by a statistical model. In this case the width for the emission of a charged particle is much less than that for the emission of a neutron, and the γ ray emission is important only when the excitation energy is smaller than the one-neutron separation energy. The survival probability of emitting x neutrons can be written as:

$$W_{\mathrm{sur}}(E^*_{\mathrm{CN}},x,J)=P(E^*_{\mathrm{CN}},x,J)\cdot\prod_i^x\left[\frac{\Gamma_{\mathrm{n}}(E_i^*,J)}{\Gamma_{\mathrm{n}}(E_i^*,J)+\Gamma_{\mathrm{f}}(E_i^*,J)}\right], \tag{18}$$

where E^*_{CN}, and J are the excitation energy and the angular momentum of the compound nucleus, respectively. E_i^* is the excitation energy before evaporating the i-th neutron, which satisfies the relation:

$$E^*_{i+1}=E_i^*-B_i^{\mathrm{n}}-2T_i \tag{19}$$

with the initial excitation energy $E_1^*=E^*_{\mathrm{CN}}$, B_i^{n} is the separation energy of the i-th neutron. T_i is the nuclear temperature before evaporating the i-th neutron and obtained from $E_i^*=aT_i^2-T$. Within the framework of the evaporation model and the Bohr-Wheeler formula[24], the widths of the i-th neutron evaporation and fission are obtained respectively by

$$\Gamma_{\mathrm{n}}(E^*,J)=\frac{2s+1}{2\pi\rho(E_i^*,J)}\frac{2M_{\mathrm{n}}R^2}{\hbar^2}\cdot\int_0^{E_i^*-B_i^{\mathrm{n}}-1/a_i}\varepsilon\,\rho(E_i^*-B_i^{\mathrm{n}}-\varepsilon,J)\mathrm{d}\varepsilon, \tag{20}$$

and

$$\Gamma_{\mathrm{f}}(E^*,J)=\frac{1}{2\pi\rho(E^*,J)}\cdot\int_0^{E_i^*-B_i^{\mathrm{f}}-1/a_{\mathrm{f}_i}}\rho(E^*-B_{\mathrm{f}}-\varepsilon,J)\mathrm{d}\varepsilon, \tag{21}$$

where

$$\rho(E_i^*,J)=\frac{1}{\sqrt{48}E^*}\exp\left\{2\sqrt{a\left[E_i^*-\frac{J(J+1)\hbar^2}{2\mathscr{J}}\right]}\right\}$$

is the level density, M_{n} and s are the mass and spin of the neutron. R, B_i^{f}, are the radius of the nucleus A_{i-1} before evaporating i-th neutron, respectively. a is the level density parameter which is taken to be $a=A/12$. In Ref.[25] the fission barrier for SHE is divided into two parts: the macroscopic part $B_{\mathrm{f}}^{\mathrm{LD}}$, determined by the liquid-drop model[26], and the microscopic part $B_{\mathrm{f}}^{\mathrm{Mic}}$, determined by shell correction. The microscopic energy will be damped due to the dependence of the shell effects on the nuclear excitation. Thus, the fission barrier can be written as:

$$B_{\mathrm{f}}=B_{\mathrm{f}}^{\mathrm{LD}}+B_{\mathrm{f}}^{\mathrm{Mic}}(E^*=0)\exp\left[-\frac{E^*}{E_{\mathrm{D}}}\right]-\left(\frac{\hbar^2}{2J_{\mathrm{gs}}}-\frac{\hbar^2}{2J_{\mathrm{sd}}}\right)J(J+1), \tag{22}$$

where E_{D} is the damping factor describing the decrease of the influence of the shell effects on the level density as the excitation energy of the nucleus increases, which is taken as

$$E_{\mathrm{D}}=\frac{0.4A^{4/3}}{a}, \tag{23}$$

where A is the mass number of the nucleus. $J_{\mathrm{gs;sd}}=k\frac{2}{5}MR^2(1+\beta_2^{\mathrm{gs;sd}}/3)$ are the moment of inertia of the fissioning nucleus at its ground state and the saddle state, respectively. Here $k\approx0.4$[27]. Since there are no data available, the quadrupole deformation parameters β_2 at the saddle point are taken from the microscopic calculation of the relativistic mean field (RMF) theory[28], which has been proven to be quite successful for the description of

exotic nuclei and SHN. In the case of the emission of x neutrons ($x>1$), the realization probability is given by the formula of neutron evaporation proposed by Jackson[29] as

$$P(E^*_{CN},x,J)=I(\Delta_x,2x-3)-I(\Delta_{x+1},2x-1)\ , \qquad (24)$$

where

$$I(z,m)=\frac{1}{m!}\int_0^z u^m e^{-u}du\ ,$$

and

$$\Delta_x=\frac{1}{T}(E^*_{CN}-\sum_{i=1}^{x}B_i^n),$$

T is the nuclear temperature. For the 1n evaporation channel, we use the expression of Eq. (7) from Ref. [25].

Taking the neutron separation energy and B_f^{Mic} from Ref. [9], the calculated survival probabilities for one-neutron emission of Pb-based reactions at nearly central collisions with the optimal excitation energies are shown in Fig. 2(b). The tendency of the results is basically consistent with that shown in Fig. 4 of Ref. [25].

In Fig. 3 we show the comparison of survival probabilities as a function of excitation energy for the reactions $^{48}Ca+^{208}Pb$ and $^{48}Ca+^{238}U$ at angular momentum $J=0\ \hbar$. The $^{48}Ca+^{208}Pb$ system has larger survival probabilities in the 1—5n evaporation channels, especially at higher excitation energies since it has non-zero macroscopic fission barrier as shown in the first part in Eq. (22).

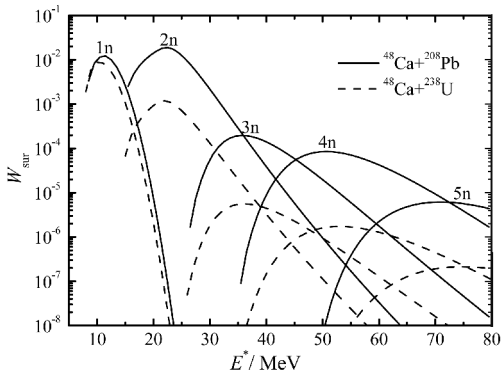

Fig. 3 The survival probabilities of the reactions $^{48}Ca+^{208}Pb$ and $^{48}Ca+^{238}U$ at angular momentum $J=0\ \hbar$ as a function of the excitation energies.

3 The Formation Probability of SHN

3.1 The evaporation residue cross section

Based on the above theory we calculated the evaporation residue cross sections. For cold fusion reactions with the optimal excitation energies, a set of evaporation residue cross sections for Pb-based reactions are shown in Fig. 4 with stars, the solid dots are experimental data quoted in Ref. [30], and some estimated data for element 114, 116, and 118 by different groups are indicated in the figure[31—33]. The upper limit for element 118 was estimated by LBNL recently[34] and also shown in this figure. Our results are in principle in agreement with the data within one order of magnitude.

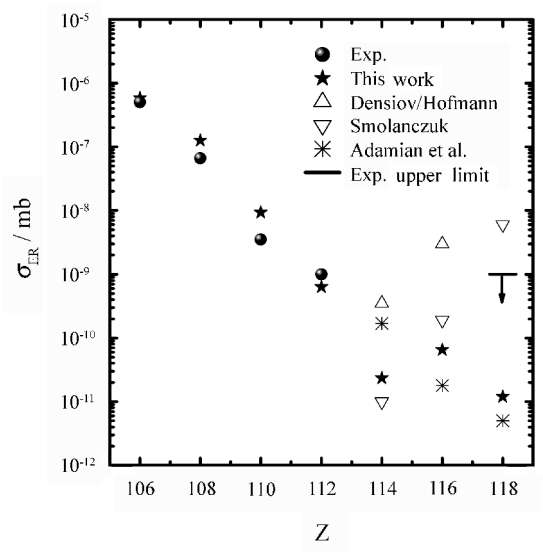

Fig. 4 The evaporation residue cross sections for one-neutron emission Pb-based reactions with the excitation energies from Fig. 2 as a function of the charge number of compound nuclei. Our calculated results are indicated by solid stars, the experimental data by solid dots. And some estimated data for element 114, 116, and 118 by different groups are indicated with different symbols.

3.2 The SHN production excitation functions from ^{48}Ca induced reactions

By introducing the barrier distribution function method in the DNS model the calculated fusion evaporation excitation functions of SHN 114 in the $^{48}Ca+^{242}Pu$ and $^{48}Ca+^{244}Pu$ reactions are shown in

Fig. 5. It indicates that it is easier to produce SHN in the 4n evaporation channel in the two reaction systems due to larger production cross sections. The experimental data taken from Ref. [35] are shown by the solid squares, open circles and solid diamonds for 3n, 4n and 5n evaporation channels, respectively. At the considered excitation energies $E^* > 25$ MeV, since the capture cross section σ_c depends weakly on E^*, the properties of the excitation functions for the 3—5n evaporation channels are mainly determined by the function P_{CN} and the distribution of the survival probability. There are small difference of the positions of the maximal of the excitation functions between the calculated results and the experimental data, which perhaps comes from the beam energy loss since the blocking

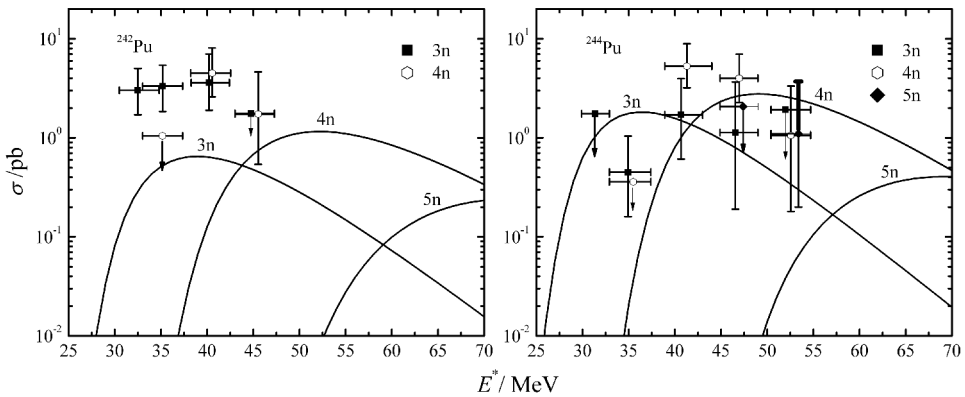

Fig. 5 Production cross sections for 2—5n evaporation channels in the reactions ^{48}Ca + ^{242}Pu and ^{48}Ca + ^{244}Pu versus the experimental data from Dubna[35].

of the target thickness. However, the values of the maximum production cross sections are in good agreement with the experimental data. The excitation functions for the 3—5n evaporation channels of SHE 116 in the ^{48}Ca + ^{248}Cm reaction are shown in Fig. 6. One can see that the 4n evaporation channel has larger production cross sections. The element 115 was synthesized at Dubna in the ^{48}Ca + ^{243}Am reaction by 3n and 4n evaporation channels[2,35]. We have calculated the evaporation residue excitation functions for the 3n and 4n evaporation channels as shown in Fig. 7. The corresponding maximum production cross sections are 4.3 and 6.8 pb for the 3n and 4n evaporation channels at excitation energies 41 and 58 MeV, respectively. Within error bars the experimental data can be reproduced very well.

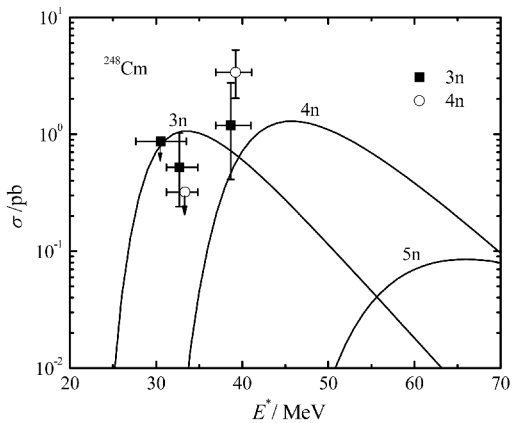

Fig. 6 Calculated production cross sections in the ^{48}Ca + ^{248}Cm reaction versus experimental data from Ref. [35].

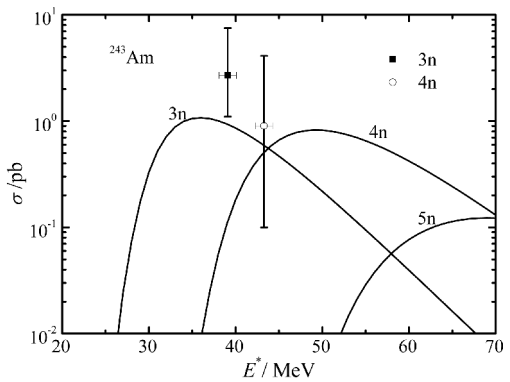

Fig. 7 The same as in Fig. 6, but for the $^{48}Ca+^{243}Am$ reaction leading to the formation of superheavy element 115 in 3n and 4n evaporation channels.

4 Summary

The fusion probability is calculated in very strongly damped reaction processes, where large amounts of the relative kinetic energy are changed into intrinsic excitation energy and nucleons transfer from the lighter fragment to the heavier one to produce the SHN in the tail of the heavy-fragment mass distribution. Within the DNS conception, instead of solving FPE analytically, the ME is solved numerically in order to calculate the fusion probability, so that the harmonic oscillator approximation to the potential energy of the DNS, which is the very essence of the nuclear structure of the model[6,12], is avoided. The nucleon transition probabilities, which are derived microscopically, are coupled with the relative motion and thus are time-dependent. Comparing with the analytical (or the logistic-type) solution of FPE at the equilibrium, our time dependent results preserve more dynamical effects. Our calculated evaporation residue cross sections for one-neutron emission channel of Pb-based reactions are basically in agreement with the experimental data within one order of magnitude. By introducing the barrier distribution function method in the DNS model a set of calculated fusion-evaporation excitation functions of SHN induced by ^{48}Ca are in good agreement with available experimental data. However, although the driving potential has been calculated in two dimensions (η and R), the diffusion process to the two dimensions is not treated simultaneously. The quasi fission is treated by a decay rate of Kramers' type. The ME should be extended into a two dimensional case by taking the distance between the centers of nuclei into account in addition, so that the quasi fission could be described in the process to fully understand the reaction dynamics.

References:

[1] Hofmann S. Rep Prog Phys, 1998, **61**: 636.

[2] Oganessian Yu Ts, Yeremin A V, Popeko A G, *et al*. Nature, 1999, **400**: 242.

[3] Bjornholm S, Swiatecki W J. Nucl Phys, 1982, **A391**: 471.

[4] Aritomo Y, Wada T, Ohta M. Phys Rev, 1999, **C59**: 796.

[5] Cherepanov E A, Volkov V V, Antonenko N V, *et al*. Nucl Phys, 1996, **A459**: 145.

[6] Adamian G G, Antonenko N V, Scheid W. Nucl Phys, 1997, **A618**: 176.

[7] Zagrebaev V L. Phys Rev, 2001, **C64**: 034 606; Phys Rev, 2003, **C67**: R061 601; Phys Rev, 2002, **C65**: 014 607.

[8] Shen Caiwann, Kosenko Grigori, Abe Yasuhisa. Phys Rev, 2002, **C59**: 061 602(R).

[9] Smolanczuk Robert. Phys Rev, 1999, **C59**: 2 634.

[10] Nörenberg W. Phys Lett, 1974, **B53**: 289.

[11] Ayik S, Schuermann B, Nörenberg W. Z Phys, 1976, **A277**: 299; Z Phys, 1976, **A279**: 145; Schuermann B, Nörenberg W, Simbel M. Z Phys, 1978, **A286**: 263.

[12] Adamian G G, Antonenko N V, Scheid W, *et al*. Nucl Phys, 1998, **A633**: 409.

[13] Antonenko N V, Cherepanov E A, Nasirov A V, *et al*. Phys Lett, 1993, **B319**: 425; Phys Rev, 1995, **C51**: 2 634.

[14] Adamian G G, Antonenko N V, Scheid W, *et al*. Nucl Phys, 1997, **A627**: 361.

[15] Li W F, Wang N, Li J F, *et al*. Euro Phys Lett, 2003, **64**: 750.

[16] Li Wenfei, Wang Nan, Jia Fei, *et al*. J Phys, 2006, **G32**: 1 143.

[17] Feng Zhaoqing, Jin Genming, Fu Fen, *et al*. Nucl Phys, 2006, **A771**: 50.

[18] Wolschin G, Nörenberg W. Z Phys, 1978, **A284**: 209.

[19] Möller P, Nix J R , Myers W D, *et al*. Atom Data and Nuclear Data Tables, 1995, **59**: 185.

[20] Wong C Y. Phys Rev Lett, 1973, **73**: 766.

[21] Li Qingfeng, Zuo Wei, Li Wenfei, *et al*. Euro Phys J , 2005, **A24**: 223.

[22] Adamian G G, Antonenko N V, Scheid W. Phys Rev, 2003, **C68**: 034 601.

[23] Grange P, Li Junqing, Weidenmüller H A. Phys Rev, 1983, **C27**: 2 063.

[24] Bohr N, Wheeler J A. Phys Rev, 1939, **56**: 426.

[25] Adamian G G, Antonenko N V, Ivanova S P, *et al*. Phys

Rev, 2000, **C62**, 064 303.
[26] Vandenbosch R, Huizenga J. Nuclear Fission. New York, London: Academic Press, 1973.
[27] Zagrebaev V I, Aritomo Y, Itkis M G, *et al*. Phys Rev, 2001, **C65**: 014 607.
[28] Zhang W, Zhang S S, Zhang S Q, *et al*. Chin Phys Lett, 2003, **20**: 1 694.
[29] Jackson J D. Can J Phys, 1956, **34**: 767.
[30] Adamian G G, Antonenko N V, Scheid W. Nucl Phys, 2000, **A678**: 24.
[31] Denisov V Yu, Hofmann S. Phys Rev, 2000, **C61**: 034 606.
[32] Smolańczuk R. Phys Rev, 2001, **C63**: 044 607.
[33] Adamian G G, Antonenko N V, Diaz-Torres A, *et al*. AIP Conf Proc, 2001, **561**: 421.
[34] Gregorich K E, Ginter T N, Loveland W, *et al*. Euro Phys J, 2003, **A18**: 633.
[35] Oganessian Yu Ts, Utyonkoy V K, Lobanov Yu V, *et al*. Phys Rev, 2004, **C69**: 021 601(R); Phys Rev, 2004, **C70**: 064 609.

重离子碰撞中超重核的形成机制*

李君清[1,2], 左 维[1,2], 冯兆庆[1], 靳根明[1,2], 赵恩广[2,3]

(1 中国科学院近代物理研究所, 甘肃 兰州 730000;
2 兰州重离子加速器国家实验室原子核理论中心, 甘肃 兰州 730000;
3 中国科学院理论物理研究所, 北京 100080)

摘 要: 在双核模型框架下, 用数值解主方程方法计算了超重核的熔合几率。明确描述了包含能量、角动量和碎片形变弛豫的相对运动, 并与核子扩散过程相耦合。因此, 用微观方法推导出的核子跃迁几率是与时间相关的。所计算的以 Pb 为靶的冷熔合超重核形成截面和以^{48}Ca 为弹核的热熔合超重核形成激发函数与已知的实验值在合理的范围内符合。

关键词: 超重核; 双核系统; 驱动势; 主方程; 全熔合

* **基金项目**: 国家自然科学基金资助项目(10505016, 10235020, 10475099, 10375001); 中国科学院知识创新工程重点方向性资助项目(KJCX2-SW-No17); 德国 DFG 基金会资助项目